Hybrid Analog and Digital Beamforming for OFDM-Based Large-Scale MIMO Systems

Foad Sohrabi and Wei Yu
Department of Electrical and Computer Engineering
University of Toronto, Toronto, Ontario M5S 3G4, Canada
Emails: {fsohrabi, weiyu}@ece.utoronto.ca

***Abstract*—Hybrid analog and digital beamforming is a promising technique for large-scale MIMO systems since it can achieve a performance close to the performance of the conventional fully-digital beamforming schemes, but with much lower hardware implementation complexity and power consumption. One of the major challenges in hybrid beamforming is to design the hybrid beamformers for broadband systems with frequency-selective channels. This is because in broadband systems, it is desirable to design the same analog beamformers for the entire band while adapting digital beamformers in each frequency tone. In this paper, we consider the hybrid beamforming design for large-scale MIMO systems with orthogonal frequency division multiplexing (OFDM) modulation. Specifically, we propose a unified heuristic design for two different hybrid beamforming structures, the fully-connected and partially-connected structures, to maximize the overall spectral efficiency of a broadband system. Numerical results show that the proposed algorithm outperforms the existing hybrid beamforming designs and further the proposed algorithm for the fully-connected structure can achieve spectral efficiency close to that of the optimal fully-digital solution with much less number of RF chains.**

I. Introduction

Investigation of the mmWave frequency spectrum for the next generation of wireless standard has recently received significant attention due to the bandwidth shortage in the conventional bandwidth spectrum that is currently used in 3G or LTE systems [1]. The pathloss and absorption in the mmWave frequency band is much higher than those in the conventional frequency bands. However, since the wavelength is shorter in high frequencies, more antenna elements can be packed in the transceivers of the mmWave systems to overcome the poor characteristics of the channel [2]. One of the challenges in designing the systems with large-scale antenna arrays is that the implementation of the conventional fully-digital beamforming schemes is not practical. This is because the fully-digital beamforming requires one dedicated RF chain per antenna element which imposes a large hardware complexity and power consumption to the system.

To reduce the number of active RF chains, this paper considers the hybrid analog and digital beamforming in which the overall beamformer is implemented by concatenation of a low-dimensional digital beamformer and a high-dimensional analog beamformer which is realized with simple analog components such as phase shifters. The hybrid beamforming design for point-to-point multiple-input multiple-output (MIMO) systems with flat fading channel model has been studied in the literature [3]–[7]. In [5], it is shown that for flat fading channels, if the number of RF chains at the transceivers is twice the number of data streams, the hybrid beamforming can exactly achieve the performance of the fully-digital beamforming. Moreover, [3]–[5] propose different heuristic hybrid beamforming designs that approach the performance of fully-digital beamforming.

Most of the existing results however are restricted to the flat fading channel model. But practical large-scale MIMO systems also need to be implemented in the broadband mmWave spectrum with frequency selective channels. This motivates us to consider the hybrid beamforming design for orthogonal frequency division multiplexing (OFDM) based large-scale MIMO systems. In particular, this paper considers designing the hybrid beamformers for two different hybrid beamforming architectures, the fully-connected and partially-connected architectures, to maximize the overall spectral efficiency under the total power constraint for each subcarrier. Toward this aim, we first find the optimal design for the digital beamformer of each subcarrier assuming the given analog beamformer. Further, by exploiting the structure of those optimal digital beamformers, we derive an upper-bound on the overall spectral efficiency that can be used to design the analog beamformer in the entire spectrum. Numerical results show that the proposed algorithm for fully-connected hybrid beamforming with relatively few RF chains can already achieve a performance close to the performance of the optimal fully-digital beamforming.

It should be mentioned that some recent work also considers the hybrid beamforming design for frequency selective channel model [8]–[10]. Among those, [10] considers the same system model as in this paper; i.e., hybrid beamforming for point-to-point MIMO systems with perfect channel state information (CSI) knowledge. In the numerical part of this paper, it is shown that the proposed method achieves a higher performance as compared to the algorithm in [10] for both fully-connected and partially-connected structures.

II. System Model

Consider a single-user OFDM-based large-scale MIMO system in which a transmitter with N_t antennas and N_{RF} transmit RF chains sends N_s data streams per subcarrier to a receiver equipped with N_r antennas and N_{RF} receive RF chains. In practice, the number of available RF chains in the large-scale MIMO systems is much smaller than the number

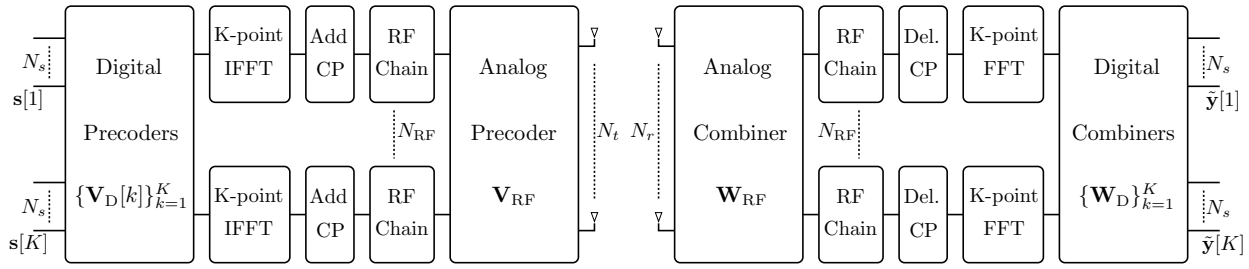

Fig. 1: A block diagram of an OFDM-based large-scale MIMO system with hybrid analog and digital beamforming architecture at the transceivers.

of transceiver antennas, i.e., $N_{\mathrm{RF}} \ll \min(N_t, N_r)$. Hence, it is not feasible to use the conventional fully-digital beamforming schemes which require one dedicated RF chain per antenna. To address the challenge of this hardware limitation, this paper considers the hybrid beamforming architecture as shown in Fig. 1 in which the overall beamformer at each end is constructed by the concatenation of a low-dimensional digital beamformer and a high-dimensional analog beamformer where that analog beamformer is implemented using simple analog components such as analog phase shifters and adders.

In OFDM-based hybrid beamforming architecture shown in Fig. 1, the transmitter first precodes N_s data streams $\mathbf{s}[k]$ at each subcarrier $k = 1, \ldots, K$, using a low-dimensional digital precoder, $\mathbf{V}_{\mathrm{D}}[k] \in \mathbb{C}^{N_{\mathrm{RF}} \times N_s}$, then transforms the processed signal to the time domain employing N_{RF} K-point inverse fast Fourier transforms (IFFTs). Finally, after adding a cyclic prefix, the transmitter uses an analog precoder, $\mathbf{V}_{\mathrm{RF}} \in \mathbb{C}^{N_t \times N_{\mathrm{RF}}}$, to construct the transmitted signal. Note that since the analog precoding is a post-IFFT process, the analog precoder is identical for all subcarriers. As a result, the transmitted signal at k^{th} subcarrier can be written as

$$\mathbf{x}[k] = \mathbf{V}_{\mathrm{RF}}\mathbf{V}_{\mathrm{D}}[k]\mathbf{s}[k], \tag{1}$$

where $\mathbf{s}[k] \in \mathbb{C}^{N_s \times 1}$ is the vector of intended symbols to the receiver at the k^{th} subcarrier, normalized such that $\mathbb{E}\{\mathbf{s}[k]\mathbf{s}[k]^H\} = \mathbf{I}_{N_s}$. Considering a block-fading channel model with additive white Gaussian noise for each subcarrier, the received signal at the k^{th} subcarrier can be modeled as

$$\mathbf{y}[k] = \mathbf{H}[k]\mathbf{V}_{\mathrm{RF}}\mathbf{V}_{\mathrm{D}}[k]\mathbf{s}[k] + \mathbf{z}[k], \tag{2}$$

where $\mathbf{H}[k] \in \mathbb{C}^{N_r \times N_t}$ and $\mathbf{z}[k] \sim \mathcal{CN}(\mathbf{0}, \sigma^2\mathbf{I}_{N_r})$ are the channel and Gaussian noise for the k^{th} subcarrier, respectively.

At the receiver side, the received signals of all subcarriers are first processed in time domain using an analog combiner, $\mathbf{W}_{\mathrm{RF}} \in \mathbb{C}^{N_r \times N_{\mathrm{RF}}}$. Then, the cyclic prefix is removed and the N_{RF} K-point fast Fourier transforms (FFTs) are applied to recover the frequency domain signals. At the end, the receiver employs an $N_{\mathrm{RF}} \times N_s$ digital combiner per subcarrier, $\mathbf{W}_{\mathrm{D}}[k]$, to obtain the final processed signal at subcarrier k as

$$\tilde{\mathbf{y}}[k] = \mathbf{W}_{\mathrm{t}}[k]^H\mathbf{H}[k]\mathbf{V}_{\mathrm{t}}[k]\mathbf{s}[k] + \mathbf{W}_t[k]^H\mathbf{z}[k], \tag{3}$$

where $\mathbf{V}_{\mathrm{t}}[k] = \mathbf{V}_{\mathrm{RF}}\mathbf{V}_{\mathrm{D}}[k]$ and $\mathbf{W}_{\mathrm{t}}[k] = \mathbf{W}_{\mathrm{RF}}\mathbf{W}_{\mathrm{D}}[k]$ are the overall hybrid precoder and combiner for the k^{th} subcarrier, respectively.

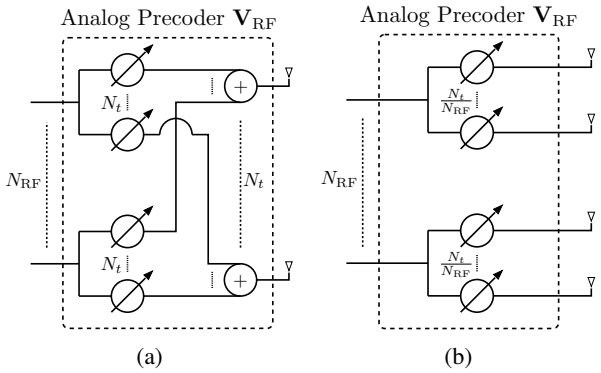

(a) (b)

Fig. 2: (a) The architecture of an analog precoder with fully-connected structure. (b) The architecture of an analog precoder with partially-connected structure.

As it is mentioned, the analog part of the hybrid beamformer is typically implemented with simple components such as analog phase shifters which can only adjust the phases of the signals. Hence, the non-zero elements of the analog beamformers should satisfy the constant modulus constraint, i.e., $|\mathbf{V}_{\mathrm{RF}}(i,j)| = |\mathbf{W}_{\mathrm{RF}}(i,j)| = 1$. Two widely-used analog beamformer architectures for hybrid beamforming are

- **Fully-connected Architecture:** In this structure, the output signal of each RF chain is sent to all the antennas after passing through a network of phase shifters as shown in Fig. 2(a). Therefore, the total number of active phase shifters in this structure is $N_t N_{\mathrm{RF}}$.
- **Partially-connected Architecture:** In this architecture, only N_t/N_{RF} portion of antennas is dedicated to transmit the different phase shifted version of the output signal of each RF chain, as shown in Fig. 2(b). This architecture implies that the analog beamformer has a block-diagonal structure, i.e., for the analog precoder,

$$\mathbf{V}_{\mathrm{RF}} = \begin{bmatrix} \mathbf{v}_1 & \mathbf{0} & \cdots & \mathbf{0} \\ \mathbf{0} & \mathbf{v}_2 & & \mathbf{0} \\ \mathbf{0} & \mathbf{0} & \ddots & \mathbf{0} \\ \mathbf{0} & \mathbf{0} & \cdots & \mathbf{v}_{N_{\mathrm{RF}}} \end{bmatrix}, \tag{4}$$

  where each element of $\mathbf{v}_i$ satisfies the constant modulus constraint. Therefore, it can be seen that the total number of phase shifters in this structure is reduced to N_t.

The fully-connected structure can achieve the full beamforming gain for the signal of each RF chain, while the partially-

connected structure can only achieve N_t/N_{RF} of the full beamforming gain. On the other hand, the hardware implementation complexity and power consumption of the partially-connected architecture are lower as compared to those of fully-connected structure. Therefore, there is a performance-complexity trade-off in choosing the above structures [10].

In this paper, for both fully-connected and partially-connected structures, we consider the problem of designing the hybrid beamformers for maximizing the overall spectral efficiency with a power budget constraint for each subcarrier assuming perfect CSI, namely,

$$\begin{aligned} \underset{\mathbf{V}_{\text{RF}},\mathbf{W}_{\text{RF}},\{\mathbf{V}_{\text{D}}[k],\mathbf{W}_{\text{D}}[k]\}_{k=1}^{K}}{\text{maximize}} \quad & \frac{1}{K}\sum_{k=1}^{K} R[k] \\ \text{subject to} \quad & \text{Tr}(\mathbf{V}_{\text{t}}[k]\mathbf{V}_{\text{t}}[k]^H) \le P, \\ & |\mathbf{V}_{\text{RF}}(i,j)| = 1, \forall \text{non-zero entires}, \\ & |\mathbf{W}_{\text{RF}}(i,j)| = 1, \forall \text{non-zero entires}, \end{aligned} \tag{5}$$

where P is the transmit power budget per subcarrier, and $R[k]$ is the overall spectral efficiency of the k^{th} subcarrier assuming Gaussian signalling, i.e.,

$$R[k] = \log_2\Big|\mathbf{I}_{N_r} + \frac{1}{\sigma^2}\mathbf{C}[k]\mathbf{H}[k]\mathbf{V}_{\text{t}}[k]\mathbf{V}_{\text{t}}[k]^H\mathbf{H}[k]^H\Big|, \tag{6}$$

where $\mathbf{C}[k] = \mathbf{W}_{\text{t}}[k](\mathbf{W}_{\text{t}}[k]^H\mathbf{W}_{\text{t}}[k])^{-1}\mathbf{W}_{\text{t}}[k]^H$, $\mathbf{V}_{\text{t}}[k] = \mathbf{V}_{\text{RF}}\mathbf{V}_{\text{D}}[k]$ and $\mathbf{W}_{\text{t}}[k] = \mathbf{W}_{\text{RF}}\mathbf{W}_{\text{D}}[k]$.

III. Hybrid Beamforming Design

This paper considers the design of hybrid precoders and combiners for the cases that $N_{\text{RF}} \ge N_s$ by solving the problem in (5). In general, solving the optimization problem (5) requires a joint optimization over the hybrid precoders and combiners. However, similar to [4], [5], this paper considers a decoupled design in which the hybrid precoders are first designed assuming that the perfect receiver is used and then the hybrid combiners are designed given the already designed hybrid precoders. Following this strategy, the transmitter design problem can be written as

$$\begin{aligned} \max_{\mathbf{V}_{\text{RF}},\{\mathbf{V}_{\text{D}}[k]\}_{k=1}^{K}} \quad & \frac{1}{K}\sum_{k=1}^{K}\tilde{R}[k] \\ \text{s.t.} \quad & \text{Tr}(\mathbf{V}_{\text{RF}}\mathbf{V}_{\text{D}}[k]\mathbf{V}_{\text{D}}[k]^H\mathbf{V}_{\text{RF}}^H) \le P \\ & |\mathbf{V}_{\text{RF}}(i,j)| = 1, \forall \text{non-zero entires}, \end{aligned} \tag{7}$$

where

$$\tilde{R}[k] = \log_2\Big|\mathbf{I} + \frac{1}{\sigma^2}\mathbf{H}[k]\mathbf{V}_{\text{RF}}\mathbf{V}_{\text{D}}[k]\mathbf{V}_{\text{D}}[k]^H\mathbf{V}_{\text{RF}}^H\mathbf{H}[k]^H\Big| \tag{8}$$

is the achievable rate on subcarrier k. The optimization problem (7) is challenging even for single-carrier systems, i.e., $K = 1$, since it is not convex [5]. In this paper, we consider the following procedure to decouple the design of the digital precoders and the analog precoder. First, we find the closed-form solution of the optimal digital precoders, $\{\mathbf{V}_{\text{D}}[k]\}_{k=1}^{K}$, that solves problem (7) for a given analog precoder, $\mathbf{V}_{\text{RF}}$. Further, we exploit the structure of the optimal digital precoder of each subcarrier and show that the term $\mathbf{V}_{\text{D}}[k]\mathbf{V}_{\text{D}}[k]^H$ in (8) can be approximated by $\gamma^2\mathbf{U}[k]\begin{bmatrix}\mathbf{I}_{N_s} & \mathbf{0}\\ \mathbf{0} & \mathbf{0}\end{bmatrix}\mathbf{U}[k]^H$ where γ is a constant and $\mathbf{U}[k]$ is a unitary matrix. Using this approximation and the concavity property of $\log_2|\cdot|$ function, we derive an upper-bound for the objective function in (7). Finally, we propose an iterative algorithm to find the analog precoder such that it locally maximizes the obtained upper-bound.

A. Digital Precoding Design

This part seeks to design the digital precoders assuming that the analog precoder is given. Under this assumption, $\mathbf{H}_{\text{eff}}[k] = \mathbf{H}[k]\mathbf{V}_{\text{RF}}$ can be seen as the effective channel for the k^{th} subcarrier. Further, it is easy to see that without loss of optimality, we can consider solving the following subproblem for designing the digital precoder of the k^{th} subcarrier instead of solving the optimization problem in (7), i.e.,

$$\begin{aligned} \max_{\mathbf{V}_{\text{D}}[k]} \quad & \log_2\Big|\mathbf{I} + \frac{1}{\sigma^2}\mathbf{H}_{\text{eff}}[k]\mathbf{V}_{\text{D}}[k]\mathbf{V}_{\text{D}}[k]^H\mathbf{H}_{\text{eff}}[k]^H\Big| \\ \text{s.t.} \quad & \text{Tr}(\mathbf{Q}\mathbf{V}_{\text{D}}[k]\mathbf{V}_{\text{D}}[k]^H) \le P, \end{aligned} \tag{9}$$

where $\mathbf{Q} = \mathbf{V}_{\text{RF}}^H\mathbf{V}_{\text{RF}}$. The problem (9) has a closed-form water-filling solution as

$$\mathbf{V}_{\text{D}}[k] = \mathbf{Q}^{-1/2}\mathbf{U}_e[k]\mathbf{\Gamma}_e[k], \tag{10}$$

where $\mathbf{U}_e[k]$ is the set of right singular vectors corresponding to the N_s largest singular values of $\mathbf{H}_{\text{eff}}[k]\mathbf{Q}^{-1/2}$ and $\mathbf{\Gamma}_e[k]$ is the diagonal matrix of allocated powers to each symbol on the k^{th} subcarrier.

Now, for large-scale antenna arrays, i.e., $N \to \infty$, we want to show that the optimal digital precoder in (10) can be approximated as $\mathbf{V}_{\text{D}}[k] \approx \gamma\mathbf{U}_e[k]$ where γ is a constant value. The following Lemma helps us to prove that.

Lemma 1. *Consider a hybrid beamforming transceiver with N antennas, N_{RF} RF chains and $\mathbf{F}_{RF}$ as the analog beamformer. For fully-connected structure, the analog beamformer typically satisfies $\mathbf{F}_{RF}^H\mathbf{F}_{RF} \approx N\mathbf{I}$ when $N \to \infty$, while the analog beamformer of a partially-connected structure exactly satisfies $\mathbf{F}_{RF}^H\mathbf{F}_{RF} = \frac{N}{N_{RF}}\mathbf{I}$.*

Proof: For hybrid beamforming with fully-connected architecture, the diagonal elements of $\mathbf{F}_{\text{RF}}^H\mathbf{F}_{\text{RF}}$ are exactly N while the off-diagonal elements can be approximated as a summation of N independent unit-norm complex numbers which implies that the norm of off-diagonal elements are much less than N with high problibility when $N \to \infty$. Therefore, $\mathbf{F}_{\text{RF}}^H\mathbf{F}_{\text{RF}}$ can be approximated by $N\mathbf{I}$ for fully-connected architecture.

For hybrid beamforming with partially-connected architecture, the diagonal elements of $\mathbf{F}_{\text{RF}}^H\mathbf{F}_{\text{RF}}$ are N/N_{RF}, while the off-diagonal elements are zero due to the block diagonal structure of the analog beamformer (as in (4)). Therefore for the partially-connected architecture, we have $\mathbf{F}_{\text{RF}}^H\mathbf{F}_{\text{RF}} = \frac{N}{N_{\text{RF}}}\mathbf{I}$. ■

Now, using Lemma 1, it can be seen that $\mathbf{Q}$ is approximately proportional to the identity matrix, i.e., $\mathbf{Q} \propto \mathbf{I}$, for both fully-connected and partially-connected structures. Further, assuming equal power allocation for all streams, i.e., $\mathbf{\Gamma}_e[k] \propto \mathbf{I}$, we have $\mathbf{V}_{\text{D}}[k] \approx \gamma \mathbf{U}_e[k]$ where γ should be chosen such that the power constraint in (9) is satisfied. Therefore, it can be shown that for fully-connected structure $\gamma = \sqrt{P/(N_t N_s)}$ and for partially-connected structure $\gamma = \sqrt{(P N_{\text{RF}})/(N_t N_s)}$. Finally, it is easy to see that such a digital precoder satisfies

$$\mathbf{V}_{\text{D}}[k]\mathbf{V}_{\text{D}}[k]^H \approx \gamma^2 \mathbf{U}[k] \begin{bmatrix} \mathbf{I}_{N_s} & \mathbf{0} \\ \mathbf{0} & \mathbf{0} \end{bmatrix} \mathbf{U}[k]^H, \qquad (11)$$

where $\mathbf{U}[k] \in \mathbb{C}^{N_{\text{RF}} \times N_{\text{RF}}}$ is a unitary matrix.

B. Analog Precoding Design

This part considers designing the analog precoder assuming that the digital precoders for all subcarriers satisfy (11). Under this assumption, i.e., $\mathbf{V}_{\text{D}}[k]\mathbf{V}_{\text{D}}[k]^H \approx \gamma^2 \mathbf{U}[k]\tilde{\mathbf{I}}_{N_{\text{RF}}}\mathbf{U}[k]^H$ where $\tilde{\mathbf{I}}_{N_{\text{RF}}} = \begin{bmatrix} \mathbf{I}_{N_s} & \mathbf{0} \\ \mathbf{0} & \mathbf{0} \end{bmatrix}$, the achievable rate of subcarrier k in (8) can be upper-bounded as

$$\begin{aligned} \tilde{R}[k] &= \log_2\Big|\mathbf{I} + \frac{\gamma^2}{\sigma^2}\mathbf{U}[k]^H \mathbf{V}_{\text{RF}}^H \mathbf{H}[k]^H \mathbf{H}[k]\mathbf{V}_{\text{RF}}\mathbf{U}[k]\tilde{\mathbf{I}}_{N_{\text{RF}}}\Big| \\ &\overset{(a)}{\leq} \log_2\Big|\mathbf{I} + \frac{\gamma^2}{\sigma^2}\mathbf{U}[k]^H \mathbf{V}_{\text{RF}}^H \mathbf{H}[k]^H \mathbf{H}[k]\mathbf{V}_{\text{RF}}\mathbf{U}[k]\mathbf{I}_{N_{\text{RF}}}\Big| \\ &\overset{(b)}{=} \log_2\Big|\mathbf{I} + \frac{\gamma^2}{\sigma^2}\mathbf{V}_{\text{RF}}^H \mathbf{H}[k]^H \mathbf{H}[k]\mathbf{V}_{\text{RF}}\Big|, \end{aligned} \qquad (12)$$

where (a) is satisfied with equality if $N_{\text{RF}} = N_s$ and (b) is obtained using the properties of the unitary matrices. Finally, an upper-bound for the objective function in (7) can be obtained as

$$\begin{aligned} \frac{1}{K}\sum_{k=1}^{K}\tilde{R}[k] &\overset{(c)}{\leq} \frac{1}{K}\sum_{k=1}^{K}\log_2\Big|\mathbf{I} + \frac{\gamma^2}{\sigma^2}\mathbf{V}_{\text{RF}}^H \mathbf{H}[k]^H \mathbf{H}[k]\mathbf{V}_{\text{RF}}\Big| \\ &\overset{(d)}{\leq} \log_2\Big|\mathbf{I} + \frac{\gamma^2}{\sigma^2}\mathbf{V}_{\text{RF}}^H \mathbf{F}_1 \mathbf{V}_{\text{RF}}\Big|, \end{aligned} \qquad (13)$$

where

$$\mathbf{F}_1 = \frac{1}{K}\sum_{k=1}^{K}\Big(\mathbf{H}[k]^H \mathbf{H}[k]\Big), \qquad (14)$$

and (c) follows (12) and (d) is due to the concavity property of $\log_2|\cdot|$ function; i.e., for a concave function $f(\cdot)$, if $\sum_i \alpha_i = 1$, then $\sum_i \alpha_i f(\mathbf{X}_i) \leq f(\sum_i \alpha_i \mathbf{X}_i)$.

Now, if we consider designing the analog precoder such that it maximizes the above upper-bound, the optimization problem for finding $\mathbf{V}_{\text{RF}}$ can be written as

$$\begin{aligned} \max_{\mathbf{V}_{\text{RF}}} \quad & \log_2\Big|\mathbf{I} + \frac{\gamma^2}{\sigma^2}\mathbf{V}_{\text{RF}}^H \mathbf{F}_1 \mathbf{V}_{\text{RF}}\Big| && \text{(15a)} \\ \text{s.t.} \quad & |\mathbf{V}_{\text{RF}}(i,j)| = 1, \forall \text{non-zero entires.} && \text{(15b)} \end{aligned}$$

It can be seen that this problem is now in the form of analog precoder design problem for single-carrier systems considered in [5]. Therefore, the same algorithm can be used for designing the analog precoder of the OFDM-based systems. In the rest of this section, we present a brief explanation of that algorithm in order to make the paper easier to follow.

In [5], the decoupled nature of the constraints in (15) is exploited to develop an iterative coordinate descent algorithm over the elements of $\mathbf{V}_{\text{RF}}$ to find the local optimal solution of (15). Mathematically, it is shown that the contribution of $\mathbf{V}_{\text{RF}}(i,j)$ to the objective of (15) can be extracted as

$$\log_2\big|\mathbf{C}_j\big| + \log_2\left(2\,\text{Re}\big\{\mathbf{V}_{\text{RF}}^*(i,j)\eta_{ij}\big\} + \zeta_{ij} + 1\right), \qquad (16)$$

where $\mathbf{C}_j = \mathbf{I} + \frac{\gamma^2}{\sigma^2}(\bar{\mathbf{V}}_{\text{RF}}^j)^H \mathbf{F}_1 \bar{\mathbf{V}}_{\text{RF}}^j$, and $\bar{\mathbf{V}}_{\text{RF}}^j$ is the sub-matrix of $\mathbf{V}_{\text{RF}}$ with j^{th} column removed, and $\eta_{ij} = \sum_{\ell \neq i}\mathbf{G}_j(i,\ell)\mathbf{V}_{\text{RF}}(\ell,j)$, and $\zeta_{ij} = \mathbf{G}_j(i,i) + 2\,\text{Re}\Big\{\sum_{m\neq i, n\neq i}\mathbf{V}_{\text{RF}}^*(m,j)\mathbf{G}_j(m,n)\mathbf{V}_{\text{RF}}(n,j)\Big\}$, and $\mathbf{G}_j = \frac{\gamma^2}{\sigma^2}\mathbf{F}_1 - \frac{\gamma^4}{\sigma^4}\mathbf{F}_1 \bar{\mathbf{V}}_{\text{RF}}^j \mathbf{C}_j^{-1}(\bar{\mathbf{V}}_{\text{RF}}^j)^H \mathbf{F}_1$. Since $\mathbf{C}_j$, ζ_{ij} and η_{ij} are all independent of $\mathbf{V}_{\text{RF}}(i,j)$, the optimal value for $\mathbf{V}_{\text{RF}}(i,j)$ assuming the other elements of $\mathbf{V}_{\text{RF}}$ are fixed is given by

$$\mathbf{V}_{\text{RF}}(i,j) = \begin{cases} \frac{\eta_{ij}}{|\eta_{ij}|}, & \text{for non-zero entries s.t. } \eta_{ij} \neq 0, \\ 1, & \text{for non-zero entries s.t. } \eta_{ij} = 0, \\ 0, & \text{otherwise.} \end{cases} \qquad (17)$$

Therefore, by starting with an initial feasible analog precoder satisfying (15b), and then sequentially updating each element of the analog precoder according to (17), the local optimal solution of (15) can be found.

C. Hybrid Combining Design

Finally, we seek to design the hybrid combiners that maximize the overall spectral efficiency in the objective function of (5) for the given overall hybrid precoders. For a fix analog combiner, the optimal design for the digital combiner of each subcarrier is the MMSE filter, i.e.,

$$\mathbf{W}_{\text{D}}[k] = \mathbf{J}[k]^{-1}\mathbf{W}_{\text{RF}}^H \mathbf{H}[k]\mathbf{V}_{\text{t}}[k], \qquad (18)$$

where $\mathbf{J}[k] = \mathbf{W}_{\text{RF}}^H \mathbf{H}[k]\mathbf{V}_{\text{t}}[k]\mathbf{V}_{\text{t}}[k]^H \mathbf{H}[k]^H \mathbf{W}_{\text{RF}} + \sigma^2 \mathbf{W}_{\text{RF}}^H \mathbf{W}_{\text{RF}}$. Since $\mathbf{W}_{\text{RF}}^H \mathbf{W}_{\text{RF}}. \propto \mathbf{I}$ (see Lemma. 1) for both fully-connected and partially-connected structures, the effective noise after the analog combiner approximately remains white. As a result, when the digital precoder of each subcarrier is set to the MMSE solution, the mutual information between the data symbols and the processed signals before digital combiner is approximately equal to the mutual information between the data symbols and the final processed signal. Hence, we can consider the following problem for designing the analog combiner,

$$\begin{aligned} \max_{\mathbf{W}_{\text{RF}}} \quad & \frac{1}{K}\sum_{k=1}^{K}\log_2\Big|\mathbf{I} + \frac{1}{\sigma^2}(\mathbf{W}_{\text{RF}}^H \mathbf{W}_{\text{RF}})^{-1}\mathbf{W}_{\text{RF}}^H \tilde{\mathbf{F}}[k]\mathbf{W}_{\text{RF}}\Big| \\ \text{s.t.} \quad & |\mathbf{W}_{\text{RF}}(i,j)|^2 = 1, \forall \text{non-zero entries}, \end{aligned} \qquad (19)$$

where $\tilde{\mathbf{F}}[k] = \mathbf{H}[k]\mathbf{V}_{\text{t}}[k]\mathbf{V}_{\text{t}}[k]^H \mathbf{H}[k]^H$. Now by using the result of Lemma 1, $\mathbf{W}_{\text{RF}}^H \mathbf{W}_{\text{RF}} \propto \mathbf{I}$, and using the concavity

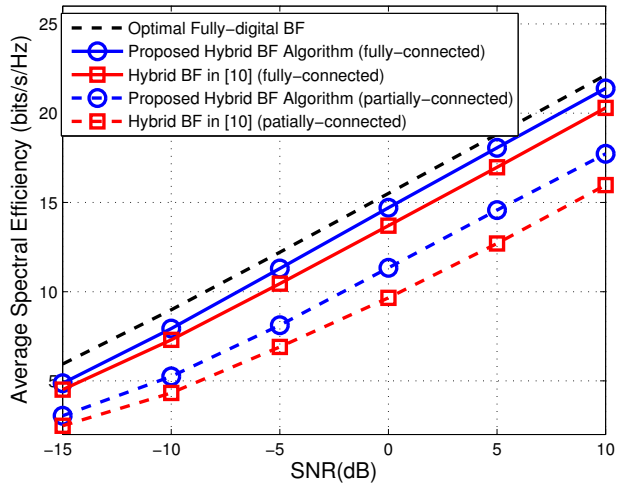

Fig. 3: Spectral efficiencies versus SNR of different methods for an 64×32 OFDM-based MIMO system with $N_s = 2$, $N_{\text{RF}} = 4$ and $K = 64$ in an environment with $N_{\text{c}} = 5$ and $N_{\text{ray}} = 10$.

property of $\log_2|\cdot|$, this paper considers maximizing the upper-bound of the objective function of (19) for designing $\mathbf{W}_{\text{RF}}$ as

$$\begin{aligned} \max_{\mathbf{W}_{\text{RF}}} \quad & \log_2\left|\mathbf{I} + \frac{1}{\sigma^2\beta}\mathbf{W}_{\text{RF}}^H\mathbf{F}_2\mathbf{W}_{\text{RF}}\right| \\ \text{s.t.} \quad & |\mathbf{W}_{\text{RF}}(i,j)|^2 = 1, \forall \text{non-zero entries}, \end{aligned} \tag{20}$$

where $\mathbf{F}_2 = \frac{1}{K}\sum_{k=1}^{K}\tilde{\mathbf{F}}[k]$, $\beta = N_r$ and $\beta = N_r/N_{\text{RF}}$ for fully-connected structure and partially-connected structure, respectively. It can be seen that this problem is in the same form as analog precoder design problem in (15). Therefore, the analog combiner $\mathbf{W}_{\text{RF}}$ can be found using the same algorithm.

IV. Simulations

In the simulation, the mmWave propagation environment is modelled as a geometric channel with N_{c} clusters and N_{ray} rays within each cluster. In such an environment, the channel matrix for the k^{th} subcarrier can be modelled as [10]

$$\mathbf{H}[k] = \sqrt{\frac{N_t N_r}{N_{\text{c}} N_{\text{ray}}}}\sum_{c=0}^{N_{\text{c}}-1}\sum_{\ell=1}^{N_{\text{ray}}}\alpha_{c\ell}\mathbf{a}_r(\phi_{c\ell}^r)\mathbf{a}_t(\phi_{c\ell}^t)^H e^{-j2\pi ck/K}, \tag{21}$$

where $\alpha_{c\ell} \sim \mathcal{CN}(0,1)$, $\phi_{c\ell}^r$ and $\phi_{c\ell}^t$ are the complex gain, angles of arrival and departure for the ℓ^{th} path in the c^{th} cluster, respectively. In the simulations, we generate the angles of arrival (departure) according to Laplacian distribution with random mean cluster angels $\bar{\phi}_c^r \in [0, 2\pi)$ ($\bar{\phi}_c^t \in [0, 2\pi)$) and angular spreads of 10 degrees within each cluster. Further, $\mathbf{a}_r(\cdot)$ and $\mathbf{a}_t(\cdot)$ are the antenna array response vectors at the receiver and the transmitter, respectively. The antenna array response vector in a uniform linear array configuration with N antennas and half-wavelength antenna spacing is modelled as $\mathbf{a}(\phi) = \frac{1}{\sqrt{N}}[1, e^{j\pi\sin(\phi)}, \ldots, e^{j\pi(N-1)\sin(\phi)}]^T$. Further, we consider a 64×32 OFDM-based MIMO system with $N_s = 2$, $N_{\text{RF}} = 4$ and $K = 64$ subcarriers in an environment with 5 clusters and 10 rays in each cluster.

Now, we numerically evaluate the performance of the proposed method as compared to the performance of the existing OFDM-based beamforming design in [10] and also to the performance of the optimal fully-digital beamforming. Note that [10] proposes two different algorithms for hybrid beamforming design in fully-connected structure. In our simulations, we implement the one (referred to "PE-AltMin" in [10]) with comparable computational complexity to our proposed algorithm which is also claimed in [10] to have better performance-complexity trade-off.

In Fig. 3, we plot the average spectral efficiency of the system against signal-to-noise-ratio in each subcarrier, $\text{SNR} = \text{P}/\sigma^2$, over 100 channel realizations for different beamforming methods. Fig. 3 shows that the proposed algorithm for both fully-connected and partially-connected structures achieves a higher spectral efficacy as compared to the hybrid beamforming algorithm in [10] which seeks to minimize the norm distance of the optimal fully-digital beamformers and the overall hybrid beamformers instead of tackling the original problem of spectral efficiency maximization. Fig. 3 also shows that the fully-connected hybrid beamforming with proposed design can approach the performance of the fully-digital beamforming with much less number of RF chains; i.e., by using only 4 RF chains at each end instead of 64 and 32 RF chains at the transmitter side and the receiver side, respectively.

V. Conclusion

This paper considers hybrid beamforming for OFDM-based large-scale MIMO systems with limited number of RF chain. A unified heuristic algorithm is proposed for designing the hybrid precoders and combiners for two well-known architectures of hybrid beamforming, fully-connected and partially-connected architectures. The simulation results verify that the proposed algorithm can achieve a better performance as compared to the existing methods for both architectures. Further, it is shown that the proposed design for fully-connected architecture can approximately achieve the performance of optimal fully-digital beamforming with much less number of RF chains.

References

[1] T. S. Rappaport, S. Sun, R. Mayzus, H. Zhao, Y. Azar, K. Wang, G. N. Wong, J. K. Schulz, M. Samimi, and F. Gutierrez, "Millimeter wave mobile communications for 5G cellular: It will work!" *IEEE Access*, vol. 1, pp. 335–349, 2013.

[2] C. H. Doan, S. Emami, D. A. Sobel, A. M. Niknejad, and R. W. Brodersen, "Design considerations for 60 GHz CMOS radios," *IEEE Commun. Mag.*, vol. 42, no. 12, pp. 132–140, 2004.

[3] X. Zhang, A. F. Molisch, and S.-Y. Kung, "Variable-phase-shift-based RF-baseband codesign for MIMO antenna selection," *IEEE Trans. Signal Process.*, vol. 53, no. 11, pp. 4091–4103, 2005.

[4] O. El Ayach, S. Rajagopal, S. Abu-Surra, Z. Pi, and R. W. Heath, "Spatially sparse precoding in millimeter wave MIMO systems," *IEEE Trans. Wireless Commun.*, vol. 13, no. 3, Mar. 2014.

[5] F. Sohrabi and W. Yu, "Hybrid digital and analog beamforming design for large-scale antenna arrays," *IEEE J. Sel. Topics Signal Process.*, vol. 10, no. 3, pp. 501–513, 2016.

[6] ——, "Hybrid beamforming with finite-resolution phase shifters for large-scale MIMO systems," in *Proc. IEEE Workshop Signal Process. Adv. Wireless Commun. (SPAWC)*, Stockholm, Sweden, Jun. 2015, pp. 136 – 140.

[7] A. Alkhateeb, O. El Ayach, G. Leus, and R. W. Heath, "Hybrid precoding for millimeter wave cellular systems with partial channel knowledge," in *Proc. Inf. Theory Appl. Workshop (ITA)*, San Diego, CA, USA, 2013, pp. 1–5.

[8] S. Park and R. W. Heath, "Frequency selective hybrid precoding in millimeter wave OFDMA systems," in *IEEE Global Commun. Conf. (GLOBECOM)*, San Diego, CA, USA, Dec 2015, pp. 1–6.

[9] A. Alkhateeb and H. R. W, "Frequency selective hybrid precoding for limited feedback millimeter wave systems," *IEEE Trans. Commun.*, 2016.

[10] X. Yu, J.-C. Shen, J. Zhang, and K. Letaief, "Alternating minimization algorithms for hybrid precoding in millimeter wave MIMO Systems," *IEEE J. Sel. Topics Signal Process.*, vol. 10, no. 3, pp. 485–500, 2016.